Highly dynamic robotic leg for non-biomimetic walking robots

Jan Baumgärtner[a], Johannes Bach[b], Lorenzo Masia[a], Essam Badreddin[a], and Peter P. Pott[b]

[a]Zentrales Institut für Informatik, Universität Heidelberg, Im Neuenheimer Feld 368, 69120 Heidelberg, Germany
[b]Institut für Medizingerätetechnik, Universität Stuttgart, Pfaffenwaldring 9, 70569 Stuttgart, peter.pott@imt.uni-stuttgart.de

Abstract

Due to a predisposition of DNA to generate symmetric anatomy, there are no tripedal animals in nature. Yet, three-legged walking might be the sweet spot between the energy efficiency of bipeds and the stability of quadrupeds. This paper presents the non-biomimetic leg for the TriPed, a novel three-legged mobile walking robot that aims to study the advantages and disadvantages of three-legged walking. We showcase its new non-biomimetic leg design that allows for fast repositioning by keeping the leg mass close to the body. This is done using physical experiments as well as a simscape simulation. The experiments show that the legs are capable of moving about 3 m/s.

1 Introduction

Although wheels are the most energy-efficient form of movement on the plane, there is no wheeled animal. This is because legs are not only used for walking but also crouching and hiding, climbing, and manipulating objects. This begs the question, how would a leg look if it was designed only for fast walking and running? This paper presents one possible design of such a leg as it is used by the TriPed robot [1]. The non-biomimetic design enables faster movements than conventional legs by keeping the main mass of the leg close to the body, with a trade-off of being more complicated leg kinematics and dynamics.

2 System Design

The TriPed is a three legged robot designed to study novel types of legged locomotion. This requires fast and responsive legs that are capable of supporting the weight of the platform. A short summary of these requirements as they pertain to the design of the leg can be seen in Table 1.

Mechanical Requirement	Value
Leg length	700 mm
Weight	30 kg
Leg angular acceleration	800 rad/s^2
Leg angular velocity	12.5 rad/s
Jump height	1 m

Table 1 Requirements for the TriPed

2.1 Leg design

The main novelties for this leg are twofold:

1. A new leg extension and retraction without a knee joint

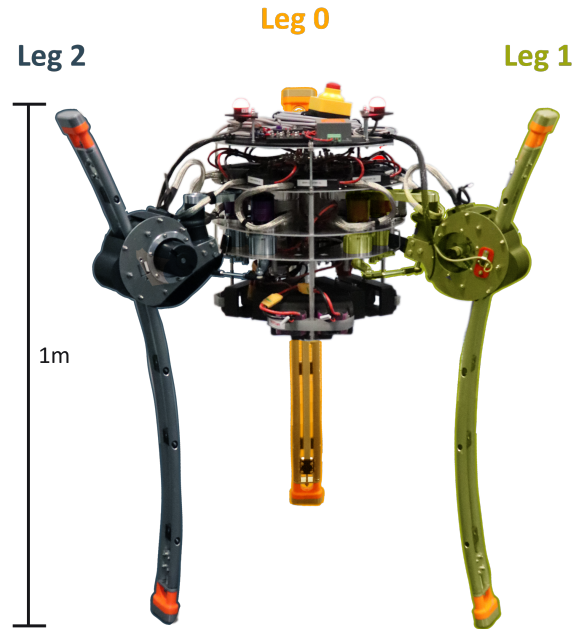2. A parallel actuated hip design

Figure 1 The threelegged TriPed robot

The main idea behind both is that walking only requires swinging the leg at the hip joint, and extending and retracting it.

2.1.1 Leg extension and retraction

In animals and conventional walking robots, extension and retraction are achieved using a knee joint. Instead, we propose a leg translation via retracting and extending the leg itself. While such leg designs were already studied by others [3] these designs were strictly passive spring dampened legs. Instead we propose a curved leg design that is actuated using a toothed belt.

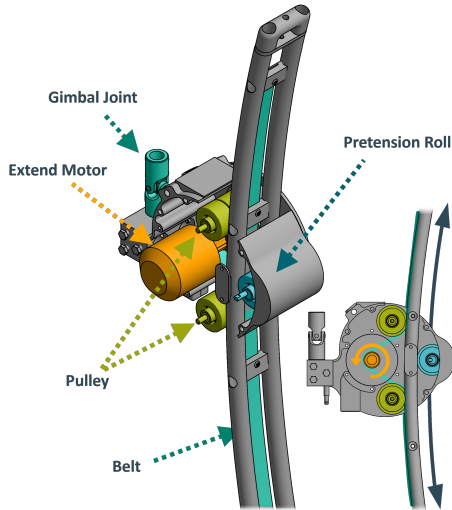The toothed belt is actuated directly without any gear

Figure 2 Leg extension mechanism

Figure 3 Leg extension sensing

Figure 4 Kinematic model of the hip

stage. Based on the specifications of a jump height of 1 m and a weight of 30 kg the maximum vertical velocity v_z of the legs has to be:

$$v_z = \sqrt{2gh} = 4.42 \ \frac{m}{s} \qquad (1)$$

Where h is the jump height and g is the gravity acceleration. With an acceleration length of 0.5 m the maximum acceleration has to be 19.5 m/s^2. Adding the gravity acceleration and multiplying with the mass of the robot one can compute the necessary motor force of all three legs to be $F_e = 879.3$ N. Each leg extension motor (*extend motor*) now has to provide a third of this force. Due to additional friction, the *extend motors* should provide 400 N of force. This force is a product of both the torque of the motors as well as the choice of tooth belt. In this sense, the curved part of the leg can be seen as a giant gear rotating around the motor. The final choice was 14 teeth which require 4.3 Nm of torque and 3788 revolutions per minute of the motors. In this case, an external rotor motor of type Flipsky 6374 (Dongguan, PRC) was used as the *extend motor*. The full mechanism can be seen in Figure 2. To measure the extension of the leg, a rotary encoder (E6A2-CW5C 500 P/R , Omron, Kyoto, JP, resolution 500 ppr, maximum frequency 30 kHz) was connected to the motor shaft. An additional photosensor of type TCST1103 (Vishay Intertechnology Inc., Milvern, PA, USA) was used to provide a reference. This photosensor is triggered by a splint embedded in a known position of the curved leg. The complate leg extension assembly can be seen in Figure 3.

2.1.2 Hip Design

To swing the leg a hip joint with two degrees of freedom is required. Here we opted for an approach where both motors are connected in parallel via a 6 bar linkage seen in Figure 4.
To estimate the torque requirements for the motors that actuate the leg motors (*swing motors*) the maximum extension of the leg was used. This leads to an actuator torque of ≈ 75 Nm. Using the maximum angular velocity of 12.5 rad/s this requires 937 W of power. This is provided by
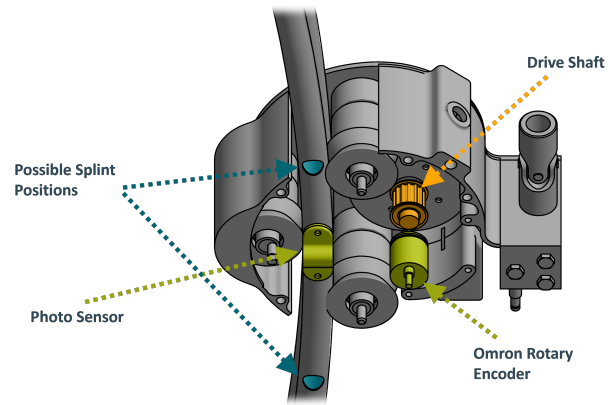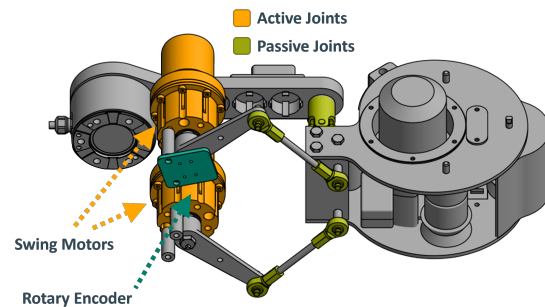
BLDC motors of type Hacker A50-16 L V4 kv 265 (Hacker Motor GmbH, Engolding, DE). Since the motor has a maximum torque of 2.47 Nm and an rpm of 10000 a 1:50 gear reduction was needed to achieve the desired performance. A harmonic drive of type CPL-20-2A (Harmonic Drive SE, Limburg-Offheim, DE) was chosen for the gear reduction. The sensing of the joint angle was achieved by AS5047D rotary encoders (Ams-Osram AG Steiermark, AT, resolution 256 ppr, maximum speed 14500 rpm) located coaxially to the output shaft of the harmonic drive.
A full overview of the leg system can be seen in Figure 5.

2.2 Chassis design

The chassis connecting the three legs can be divided into 3 layers as well as a battery bay. An overview of the chassis layers can be seen in Figure 6. The top layer houses the control computers (beaglebone black, Texas Instruments, Dallas, TX, USA) that control the joints of each leg. The motor controller houses the nine Hercules m50 motor controllers (Hacker Motor GmbH) setting the torque of each motor. The motor layer houses the *swing motors* and the bridges which connect the leg to the hip via a gimbal joint. The bottom layer houses the robots power supply.

2.3 Kinematic Modeling

The leg of the TriPed contains a serial as well as a parallel mechanism, making this a hybrid kinematic system. A common approach in the kinematic calculation of such systems is to first treat the system as a serial chain with map-
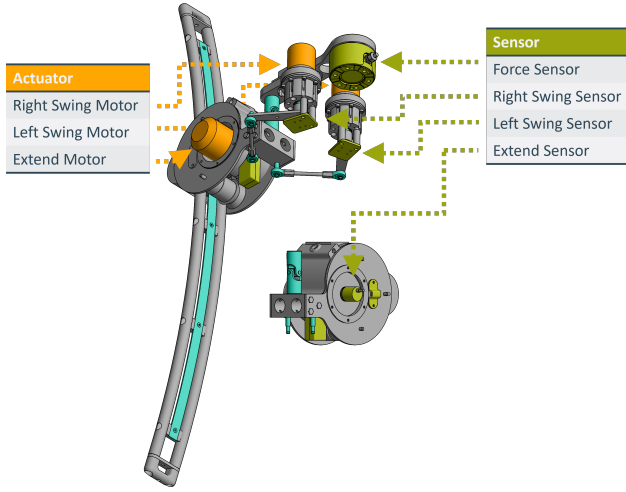
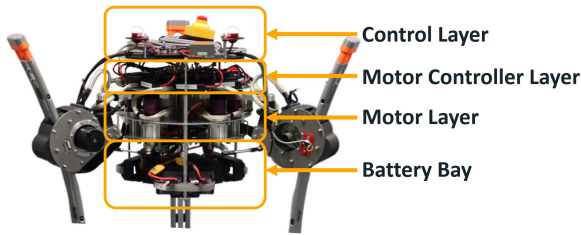**Figure 5** Schematic assembly of a single leg

Figure 6 Overview over the chassis layers

ping functions between the state of the serial chain and the actuated joints. In the case of the TriPed, this means forward kinematics are computed by:

1. Computing the angles of the gimbal joint from the angles of the *swing motor* joints

2. Compute the forward kinematics of the serial chain defined by the leg extension and the gimbal joint

Inverse Kinematics conversely are computed by:

1. Computing the inverse kinematics of the serial chain defined by the leg extension and the gimbal joint

2. Computing the angles of the *swing motor* joints from the angles of the gimbal joint

The kinematic calculations were performed by the library trip_kinematics [2], which was built for this kinematic approach.

2.3.1 Serial Chain of the TriPed

The serial chain can be divided into two parts. The first is the transformation A_p^{ccs} from the center coordinate system (ccs) to the follower frame of the gimbal joint (p frame). The second part models the rotation of the curved leg. This can be treated as if the leg would rotate around a point 150 mm away from the leg. The second part is thus defined by a transformation to the virtual center of rotation (ll-joint) and a transformation from the joint to the foot coordinate system (fcs). The full kinematic model can thus
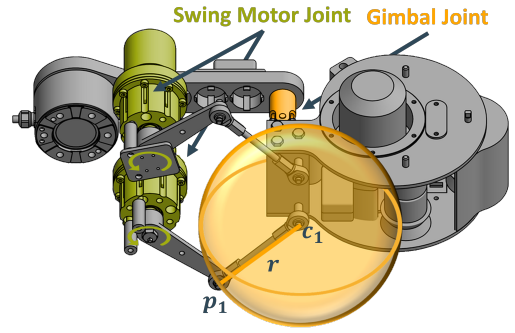

Figure 7 Geometric interpretation of the coupling rods

be defined as:

$$A_{fcs}^{ccs} = A_p^{ccs}(\mathbf{q}_{gimbal})A_{ll-joint}^{p}A_{fcs}^{ll-joint}(q_{ll}) \tag{2}$$

Where $\mathbf{q}_{gimbal}$ is the state of the gimbal joint and q_{ll} is the angle of the revolute joint at the virtual center of rotation. The precise definition of each transformation can be found in [5]. The state of the virtual center of rotation can be computed from the state of each *extend motor* joint q_e using:

$$\dot{q}_{ll} = -\dot{q}_e \frac{0.07}{2\pi 1.5} \tag{3}$$

With the position of the splint being defined at $q_{ll} = 0.1\pi$ rad.

2.3.2 Mapping between Gimbal joint and Swing motor joints

The kinematics of a closed kinematic chain can be described using a closure equation [6]

$$g(\mathbf{q}) = 0 \tag{4}$$

where $\mathbf{q}$ is the state of all the joints of the chain. Converting between the gimbal joint and swing motor joints thus means inserting the known joint state while solving for the other. The conventional analytic closure equation also requires solving for the state of all the passive joints of the assembly. To simplify this process the coupling rod between the drive module holding the *extend motor* and the output levers of the *swing motors* can be treated geometrically. The new formulation abstracts the two spherical joints of the coupling rod into the intersection of a sphere, with center $\mathbf{c}$ and a point $\mathbf{p}$. This geometric interpretation is illustrated in Figure 7. The closure equation can thus be written as:

$$g(\mathbf{q}_{gimbal}, q_{s_1}, q_{s_2}) = \sum_{i=1}^{2}(||\mathbf{p_i}(q_{s_i}) - \mathbf{c_i}(\mathbf{q}_{gimbal})|| - r^2)^2 \tag{5}$$

Where $\mathbf{q}_{gimbal}$ is the joint state of the gimbal joint and q_{s_1} and q_{s_2} are the states of the two *swing motor* joints respectively. The solving of this equation is performed numerically for both forward and inverse kinematics. The code can be found in the tutorial site of the trip_kinematics documentation [2].
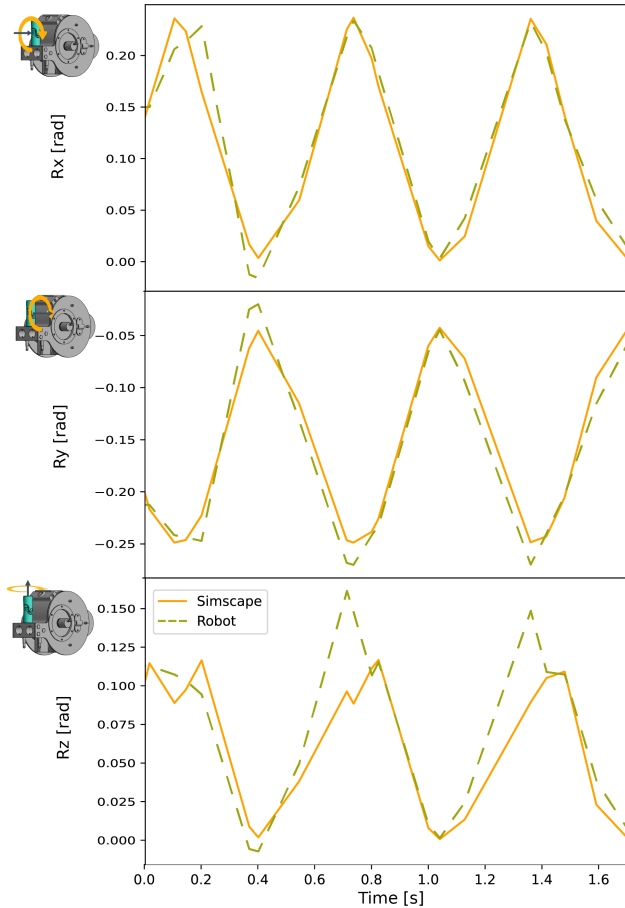
Figure 8 Comparison of Simscape hip angles and actual hip angles

3 Materials and Methods

To showcase the dynamic performance of the leg a simple experiment was set up in which the leg was tasked with reaching a set of predefined Euler angles (XYZ convention) relative to the platform. We compared the results of the physical system with a Simscape (The Mathworks, Natick, MA, USA) multibody simulation to investigate the influence of real-life dynamics.

4 Results

The results of both measurements can be seen in Figure 8. Comparing the behavior of the simulation and the robot it becomes clear that while the general shapes of the curves are similar, discrepancies in the extrema of the curves are obvious. These range from ≈ 0.02 rad for Rx and Ry to ≈ 0.064 rad for Ry.

5 Discussion

A possible reason for the angle deviations are the nonlinear dynamics of the open chains, causing the the leg mass to disturb the *swing motors* at fast direction changes. This is especially apparent in the rotation around the z Axis because the mass tends to twist the kinematic structure. For-

tunately, this twist only rotates the foot and thus causes minimal foot displacements. Future works aim to improve the dynamic leg behavior problem using a feed-forward compensation.

An additional dynamic phenomenon the physical system suffers from is vibrations of the curved leg. This is due to a trade-off between lower belt tension making the leg easier to retract and higher belt tension inhibiting vibrations.

In terms of speed, one can see that the leg is capable of changing the angle with about $4 \frac{rad}{s}$. While this is decidedly slower than the actuator speed of $12.5\frac{rad}{s}$ this was only because the speed was limited due to safety concerns. Future work will therefore focus on the safety monitoring and control that will enable the system to reach its full potential. However, even the actual slower speed is capable of moving the legs at about $3 \frac{m}{s}$. To give a comparison, this would enable a maximum movement speed at almost double the $1.6 \frac{m}{s}$ movement speed of the popular quadrupedal robot Spot by Boston Dynamics [4].

In summary, the experiments indicate that leg designs for walking robots may not have to be inspired by nature. The results at least indicate using our non-biomimetic leg design can yield fast leg movement. This is in all likelihood mainly due to the main actuators and sensors being located close to the body. This means that the curved leg itself has low inertia. Additionally connecting the hip motors in parallel means that the motors do not have to carry the weight of each other.

However, the results also indicate that the new hip design introduces nonlinearities that have to be accounted for in the joint control. At the same time, closed chains offer much higher stiffness and since any error in the orientation of the leg propagates over the full extension of the leg, a high stiffness is paramount. Future work aims to access the leg performance during actual walking.

6 Literature

[1] Bach, J.: Design, Design, construction and charateriation of a non-mimetic walking robot. Masterthesis, 2020, Institute of Medical Device Technology, University of Stuttgart

[2] Baumgärtner, J.: TriP: A Python package for the kinematic modeling of serial-parallel hybrid robots. Journal of Open Source Software. Vol. 7 No. 71, 2022, pp. 3967

[3] Ahmadi, M., Buehler, M.: Preliminary experiments with an actively tuned passive dynamic running robot. The 5th international symposium pm experimental robotics (ISER) (eds Casals, A, DeAlmeida, AT), Barcelona, Spain, 1997, pp. 313–324.

[4] support.bostondynamics.com/s/article/Robot-specifications accessed on 31.3.22

[5] https://triped-robot.github.io/docs/kinematics/ accessed on 31.3.22

[6] Kumar, S.: Modular and analytical methods for solving kinematics and dynamics of series-parallel hybrid robots. PhD thesis Universität Bremen. 2019